*Article*

# A Fractional Order Controller for Sensorless Speed Control of an Induction Motor

**Tayyaba Nosheen** [1,2], **Ahsan Ali** [1], **Muhammad Umar Chaudhry** [3,*], **Dmitry Nazarenko** [4], **Inam ul Hasan Shaikh** [1], **Vadim Bolshev** [4,5,*], **Muhammad Munwar Iqbal** [6], **Sohail Khalid** [2] **and Vladimir Panchenko** [7]

[1] Department of Electrical Engineering, University of Engineering and Technology, Taxila 47070, Pakistan
[2] Department of Electrical Engineering, Riphah International University, Islamabad 45210, Pakistan
[3] Department of Computer Science, MNS-University of Agriculture, Multan 66000, Pakistan
[4] Laboratory of Intelligent Agricultural Machines and Complexes, Don State Technical University, 344000 Rostov-on-Don, Russia
[5] Federal Scientific Agroengineering Center VIM, 109428 Moscow, Russia
[6] Department of Computer Science, University of Engineering and Technology, Taxila 47070, Pakistan
[7] Department of Theoretical and Applied Mechanics, Russian University of Transport, 127994 Moscow, Russia
**\*** Correspondence: umar.chaudhry@mnsuam.edu.pk (M.U.C.); vadimbolshev@gmail.com (V.B.);
Tel.: +92-336-6034688 (M.U.C.); +7-499-174-8595 (V.B.)

**Abstract:** Agriculture activities are completely dependent upon energy production worldwide. This research presents sensorless speed control of a three-phase induction motor aided with an extended Kalman filter (EKF). Although a proportional integral (PI) controller can ensure tracking of the rotor speed, a considerable magnitude of ripples is present in the torque generated by a motor. Adding a simple derivative to have a proportional integral derivative (PID) action can cause a further increase in ripple magnitude, as it allows the addition of high-frequency noise in the system. Therefore, a fractional-order-based PID control is presented. The proposed control scheme is applied in a closed loop with the system, and simulation results are compared with the PID controller. It is evident from the results that the fractional order control not only ensures 20 times faster tracking, but ripple magnitude in torque was also reduced by a factor of 50% compared to that while using PID and ensures the effectiveness of the proposed strategy.

**Keywords:** sensorless control; extended Kalman filter; fractional order control; fractional calculus; non-integer integral-differential equations

## 1. Introduction

The arrival of electric motors helped the world in moving towards automation. Electric motors, especially induction motors (IMs), play a vital role in the field of electrical engineering due to that the induced voltage in the rotor results in a rotor current without any physical contact with the rotor windings. Due to the wide range of industrial applications, speed control to date is an important aspect of IMs.

Induction motors are known for their robustness, reliability, and efficiency, making them well-suited for use in harsh and outdoor environments. IMs also require less maintenance compared to other types. Induction motors are widely used in the agricultural industry to power various types of equipment, such as pumps, conveyors, and fans. They are particularly useful in irrigation systems, where they are used to power large pumps that draw water from wells or rivers and distribute it to the crops. Aside from that, they are also used to power grain elevators, threshers, and other machinery used in crop processing [1,2]. Induction motors can be connected to the power take-off (PTO) shaft of a tractor to drive various types of equipment such as plows, harrows, and mowers.

## 2. Literature Review

Considering the importance in terms of their application in industry, a variety of control strategies have been proposed in the literature for speed control of the IMs. A brief survey of different control approaches namely, Scalar control, Direct self-control, and Direct torque control (DTC), has been presented in [3]. In this research, scalar and field-oriented control problems of IM are moderately solved by vector control techniques (VCTs). The control design approach for IMs being used in heating, air conditioning, and ventilation has been presented in [4]. Critical analysis of torque ripples, tracking speed, control algorithm complexity parameter variation, and switching loss is presented in [5]. Field-oriented control (FOC) for the field weakening region of the IM is presented in [6]. The FOC is used to provide a parameter dependent control of torque and flux of the IM which can then be used in speed control of the motor. The main limitation of this work comes from the dependency of the approach on system parameters. A slight change in the motor parameters can cause instability in the system. To achieve high switching frequency, Direct self-control (DSC) is presented in [7]. DSC is similar to direct torque control (DTC) except one needs to achieve DTC by controlling the rotor flux.

In Ref. [8], a high-efficiency speed control approach for IM is presented. The basic principle of this operation involves employing a switching table for the selection of the output voltage of the inverter. In [9], hysteresis controllers are designed for stator flux and torque control for IM. The limitations of the controllers proposed in [9] include the presence of high-frequency ripples and the ability to achieve reference tracking of motor speed for a relatively shorter range. To address the aforementioned issues, DTC [10,11] multilevel converters [12,13] and model predictive control (MPC) [14] have been presented for IMs. A cascaded free control structure to reduce the complexity of MPC is presented in [15].

The space vector modulation technique for direct torque control was introduced in 1992, and since then, various structures have been proposed in the literature [16]. A PI controller is used to generate a suitable voltage vector with torque variation. A stator flux-oriented control strategy is presented in [17,18]. Instead of a hysteresis controller for generating voltage components, two PI controllers are used, and a sensorless algorithm is applied to estimate flux torque. This approach is used to minimize the cost of the installation of sensors and cabling. In [19], a PI controller with two different tuning approaches is used: one is symmetric optimum, and the other is root locus. The simulation results are validated through experimentation. In [20], an indirect field-oriented control technique is implemented on the induction motor. A proportional integral derivative controller is designed by researchers, and the controller parameter is tuned by the numerical method.

Aside from speed control, various techniques are also presented in the literature for speed estimation. A comparative study based on non-linear estimators is presented in [21]. In Ref. [22], a sliding-mode observer is used to estimate the motor's states. The dynamic model of the motor is presented in a dual frame of reference. In this paper, the low-speed region is controlled without using the signal injection technique [23]. An adaptive controller with an accurate model is created. Adaptive feedforward control compensates for uncertainty and non-linear factors. A comparative analysis is presented with three control approaches. The presented control technique is complex in structure and cannot be implemented for low-cost applications. A high-order sliding mode control technique twinning with an adaptive observer is proposed in [24]. The adaptive observers are highly dependent on the motor parameters and are not stable [25,26]. They provide motor control without mechanical sensors. The main drawback of this approach is a static error that is proportional to speed. In Ref. [27], a novel observer is developed for the linear system based on fuzzy logic. The Taylor series linearizes the fifth-order non-linear model of an induction motor. The T-S fuzzy model and observer were presented in this paper. Exponential convergence of estimation errors is also achieved in this study. Experimental results validate speed tracking. In Ref. [28], the rotor position is estimated using an adaptive filter. Furthermore, a reduction in the complexity of the mathematical model of a motor is also presented.

In Ref. [29], a simple flux regulation method is presented as a solution for the induction motor's low speed and no speed issues. A constant switching frequency controller is proposed in this paper. This research reduces the flux drop issues due to hysteresis control and offers a wide speed range of control.

*Contributions of the Proposed Work*

The significant contributions of this work have been listed as follows:

1. Speed control of an induction motor by designing three fractional order controllers for flux, speed, and torque along with space vector modulation (SVM) for ripple reduction.
2. Reference speed tracking, which provides tracking with less rise time, settling time, and overshoot Speed tracking covers a wide range, e.g., low to high, high to low, and again high. The speed reversal tracking (anti-clockwise rotation) of the three-phase induction motor is also highlighted.
3. The state estimation concept for a sensor-free system is provided. The induction motor model is extended by adding two more states: speed and load torque. The EKF estimator is designed for sensorless control, which provides ideal filtering of noise and estimates states with minimal error.

The paper is organized as follows: Section 2 describes the induction motor model used in speed control. Section 3 illustrates the control strategy of the induction motor. Sections 4 and 5 demonstrate the EKF and SVM techniques used in research, respectively. Simulated results are discussed in Section 6, and a brief conclusion is presented in Section 7.

## 3. Three-Phase Induction Motor

In this research, a three-phase squirrel-cage induction motor is considered where stationary reference frames are employed. In this frame of reference, the rotor winding is fixed to the frame and thus appears stationary. Using [25,30], equations from (1)–(16) are achieved. The winding on the *d-q* axis is designated as *ds*, *dr*, *qs*, and *qr*. The direct and quadrature axes of a three-phase induction motor are shown in Figure 1. Voltage and flux linkage equations can be given as [25]:

$$V_{ds} = R_s i_{ds} + \dot{\psi}_{ds} - \psi_{qs}\omega_r \tag{1}$$

$$V_{qs} = R_s i_{qs} + \dot{\psi}_{qs} + \psi_{ds}\omega_r \tag{2}$$

$$V_{dr} = R_r i_{dr} + \dot{\psi}_{dr} \tag{3}$$

$$V_{qr} = R_r i_{qr} + \dot{\psi}_{qr} \tag{4}$$

Flux-linkage Equations:

$$\psi_{ds} = L_s i_{ds} + L_m i_{dr} \tag{5}$$

$$\psi_{qs} = L_s i_{qs} + L_m i_{qr} \tag{6}$$

$$\psi_{dr} = L_r i_{dr} + L_m i_{ds} \tag{7}$$

$$\psi_{qr} = L_r i_{qr} + L_m i_{qs} \tag{8}$$
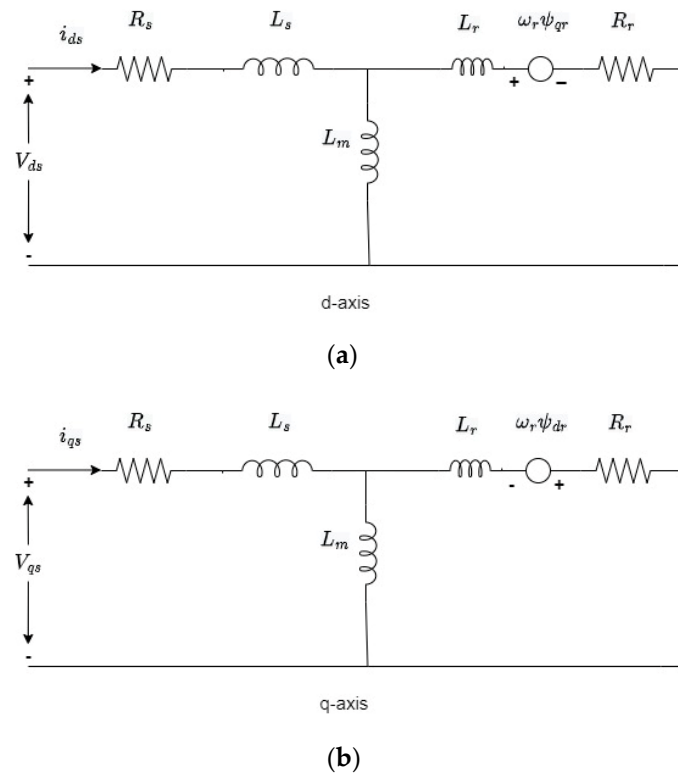
**(a)**



**(b)**

**Figure 1.** Axes of three−phase induction motor: (**a**) Direct, (**b**) Quadrature.

*State Space Model*

The time-dependent model of the induction motor can be given by Equations (9) and (10) where stator components, current, and flux are the state variables [25].

$$\dot{x}(t) = Ax(t) + Bu(t) \tag{9}$$

$$y(t) = Cx(t) \tag{10}$$

where,

$$x(t) = \begin{bmatrix} i_{s\alpha} \\ i_{s\beta} \\ \psi_{s\alpha} \\ \psi_{s\beta} \end{bmatrix}, \ y(t) = \begin{bmatrix} i_{s\alpha} \\ i_{s\beta} \end{bmatrix}$$

$$A = \begin{bmatrix} a_1 & -\omega_r & a_2 & \omega_r a_3 \\ \omega_r & a_1 & -\omega_r a_3 & a_2 \\ -R_s & 0 & 0 & 0 \\ 0 & -R_s & 0 & 0 \end{bmatrix} \tag{11}$$

$$B = \begin{bmatrix} a_4 & 0 \\ 0 & a_4 \\ 1 & 0 \\ 0 & 1 \end{bmatrix}, \ C = \begin{bmatrix} 1 & 0 \\ 0 & 1 \\ 0 & 0 \\ 0 & 0 \end{bmatrix}^T \tag{12}$$

where

$$a_1 = -\left(\frac{R_s}{\sigma L_s} + \frac{R_r}{\sigma L_r}\right), a_2 = \frac{R_s}{\sigma L_s L_r}, a_3 = \frac{1}{\sigma L_r}, \ a_4 = \frac{1}{\sigma L_s} \ and \ \sigma = 1 - \frac{L_m^2}{L_s L_r}$$

The torque equation is defined as:

$$T_e = P\left(\psi_{s\alpha} i_{s\beta} - \psi_{s\beta} i_{s\alpha}\right) \tag{13}$$

The rotating speed of the stator magnetic field can be given as:

$$N_s = \frac{120 \times f}{n} \tag{14}$$

$$\dot{\omega}_r = \frac{1}{J}\left[T_e - T_L - f_r \omega_r\right] \tag{15}$$

A list of nomenclature used in this work is given in Table 1 at the beginning of the paper and the values of motor parameters are provided in Table 2.

**Table 1.** List of parameters.

| Symbols | Description |
|---|---|
| $i_{s\alpha}$ | Stator current along the alpha axis |
| $i_{s\beta}$ | Stator current along the beta axis |
| $i_{ds}$ | Stator current along the direct axis |
| $i_{qs}$ | Stator current along the quadrature axis |
| $\psi_{s\alpha}$ | Stator flux along the alpha axis |
| $\psi_{s\beta}$ | Stator flux along the beta axis |
| $\psi_{ds}$ | Stator flux along the direct axis |
| $\psi_{qs}$ | Stator flux along the quadrature axis |
| $V_{ds}$ | Stator voltages along the direct axis |
| $V_{qs}$ | Stator Voltage along quadrature axis |
| $i_{dr}$ | Rotor current along the direct axis |
| $i_{qr}$ | Rotor current along the quadrature axis |
| $\psi_{dr}$ | Rotor flux along the direct axis |
| $\psi_{qr}$ | Rotor flux along the quadrature axis |
| $V_{dr}$ | Rotor voltages along the direct axis |
| $V_{qr}$ | Rotor voltages along quadrature axis |
| $\sigma$ | Blondel's coefficient |
| $T_e$ | Electromagnetic torque |
| $T_L$ | Load torque |
| $\omega_r$ | Rotor speed |
| $n$ | Number of poles |
| $f$ | Frequency |
| $V_{DC}$ | DC-bus voltage |

**Table 2.** Motor parameters [25].

| Parameter | Symbol | Value | Unit |
|---|---|---|---|
| Resistance of stator | $R_s$ | 6.75 | $\Omega$ |
| Resistance of rotor | $R_r$ | 6.21 | $\Omega$ |
| Inductance of stator | $L_s$ | 0.51 | H |
| Inductance of rotor | $L_r$ | 0.5192 | H |
| Mutual inductance | $L_m$ | 0.4957 | H |
| Friction coefficient | $f_r$ | 0.002 | Nm/rad |
| Inertia coefficient | $J$ | 0.01240 | kg m$^2$ |
| Poles | $p$ | 2 | - |
| Power | $P$ | 1.1 | kW |

## 4. Control Strategy

Despite the arrival of many effective design methods in the control field, PID controllers are undeniably adopted in industrial settings. The primary reason for the excessive use of PID in the industry is its cost-benefit ratio. In this research, fractional order proportional integral derivative (FOPID) and PI controllers are used for speed, flux, and torque

control. To apply the controllers in the closed loop, a stator flux-oriented control strategy is adopted in this work. Torque is aligned to the quadrature axis, while the stator flux vector is aligned along the direct axis, maintaining the quadrature component of stator flux at zero. The global control strategy is done by following the steps given below:

1. The estimated torque, speed, and flux signal are subtracted from the reference signal.
2. The difference between the reference and estimated signal (error signal) is then acting as input to the controller.
3. The reference signal is converted into (α, β) coordinate system. Using Clark transformation and the knowledge of line voltage, current, and voltage in a stationary frame of reference are obtained. Clark and Inverse Clark transformation matrices are given in (16) and (17).
4. After modulation, the signal is then fed into the inverter.

The control scheme is shown in Figure 2.

$$\begin{bmatrix} v_\alpha \\ v_\beta \end{bmatrix} = \begin{bmatrix} 0.66 & 0.33 & -0.33 \\ 0 & 0.57 & -0.57 \\ 0.33 & 0.33 & 0.33 \end{bmatrix} \begin{bmatrix} v_a \\ v_b \\ v_c \end{bmatrix} \tag{16}$$

Inverse Clark transformation is used to achieve three-phase voltages [30].

$$\begin{bmatrix} v_a \\ v_b \\ v_c \end{bmatrix} = \begin{bmatrix} cos\theta & -sin\theta & 1 \\ cos\left(\theta - \frac{2\pi}{3}\right) & -sin\left(\theta - \frac{2\pi}{3}\right) & 1 \\ cos\left(\theta + \frac{2\pi}{3}\right) & -sin\left(\theta + \frac{2\pi}{3}\right) & 1 \end{bmatrix} \begin{bmatrix} v_\alpha \\ v_\beta \end{bmatrix} \tag{17}$$
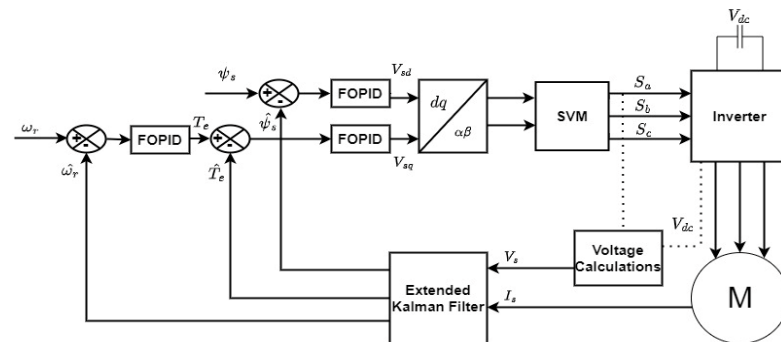


**Figure 2.** Proposed control Strategy using extended Kalman filter.

*Fractional−Order Controller*

Fractional order Derivatives are frequently used to deal with any order of integral or derivative. Among different kinds of definitions of derivatives and integrals, commonly used definitions are Grünwald−Letnikov, Riemann-Liouville, and Caputo. Using Euler's gamma function, the integer order is introduced by Riemann and Louisville [31], which defines the fractional order derivative as:

$$_aD_t^\alpha f(t) = \frac{1}{\Gamma(n-\alpha)} \frac{d^n}{dt^n} \int_a^t \frac{f(\tau)}{(t-\tau)^{\alpha-n+1}} d\tau, n-1 < \alpha < n, \tag{18}$$

where $a$ and $t$ are the upper and lower bounds respectively, $\alpha$ is the order of derivative and the operator $_aD_t^\alpha$ is the fractional differentiation or integrals [31,32]. The Laplace transform technique is used to find the continuous time transfer function of integer-order systems. The Laplace transform of the signal for an nth-order derivative can be given by (19) [31].

$$L\{D^n x(t)\} = \int_0^\infty e^{-st} {}_0D_t^n x(t)dt = s^n X(s) - \sum_{k=0}^{m-1} s^k {}_0D_t^{n-k-1}x(t)\big|_{t=0} \tag{19}$$

where $n$ has the range defined as $m - 1 < n < m$ and m belongs to Z [33]. Oustaloup presented the concept of employing a fractional order controller for a dynamic system. The Oustaloup method is one of the real-time approximation techniques that uses a recursive distribution of poles and zeroes. The transfer function based on Oustaloup's method in the given frequency range $[\omega_l \, \omega_h]$ is given in (20).

$$s^v \approx k \prod_{n=1}^{N} \frac{1 + \frac{s}{\omega_{z,n}}}{1 + \frac{s}{\omega_{p,n}}} \tag{20}$$

In the approximation, order plays an important role in the performance of the approximating transfer function. The value of gain is trained in such a way that the overall gain of the transfer function is maintained at 1 rad/s. Gain and phase dynamics are distorted by low-order approximations. Higher orders of N can be utilized to eliminate ripples [34]. The approximate method will necessitate more processing power. In (20), the pole and zero frequencies are stated by the following set of equations [34]:

$$\omega_{z,1} = \omega_l \sqrt{\eta} \tag{21}$$

$$\omega_{p,n} = \omega_{z,n}\varepsilon, n = 1, \ldots, N \tag{22}$$

$$\omega_{z,n+1} = \omega_{p,n}\eta, n = 1, \ldots, N - 1 \tag{23}$$

$$\varepsilon = \left(\frac{\omega_h}{\omega_l}\right)^{\frac{v}{N}} \tag{24}$$

$$\eta = \left(\frac{\omega_h}{\omega_l}\right)^{\frac{1-v}{N}} \tag{25}$$

The value of $v$ plays an important role in approximation e.g., when it is less than 0, the equation behaves as an inverting equation and If $|v| > 1$, the estimate is not accurate enough. As a result, it is necessary to approximate $\delta$ in (26).

$$s^v = s^n S^\delta, n \in Z, \delta[0, 1] \tag{26}$$

$$G_c(s) = K_p + K_i s^{-\lambda} + K_d s^\mu \tag{27}$$

Three parameters $K_p$, $K_i$, $K_d$ and two orders $\mu, \lambda$ with non-integer values should be optimized while constructing a FOPID controller. Taking $(\mu, \lambda) = (1, 1), (1, 0), (0, 1), (0, 0)$, the classical controllers PID, PI, PD, and P are obtained. Figure 3a [35] shows the results obtained through the classical controller. These traditional varieties of PID controllers are all variations of the FOPID controller. Figure 3b [35] demonstrates how the fractional order controller expands upon the traditional PID controller and spreads from a point to a plane. This extension may provide and increase the controller's versatility in more precisely establishing control, objectives, and actual processes.
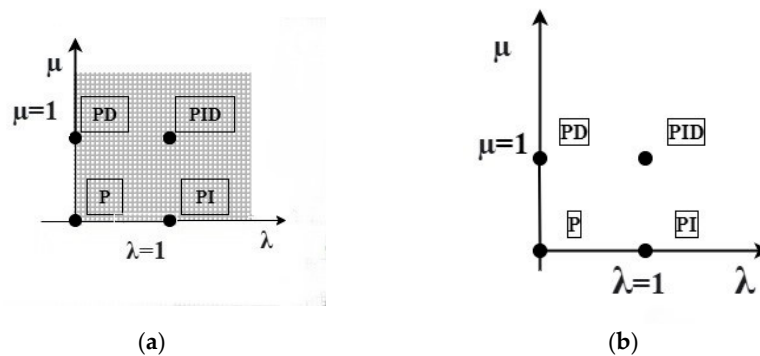


**Figure 3.** PID: (**a**) Classical order; (**b**) Fractional order.

## 5. Extended Kalman Filter (EKF)

In estimation theory, EKF is a non-linear filter used to estimate the non-linear states of systems. The Kalman filter algorithm is optimal in terms of minimizing the variance of the error estimation. It directly deals with system errors and treats them as noise. In the case of a three-phase induction motor, if speed is a state variable, then the state model becomes non-linear, so a suitable estimator for such non-linear systems is the EKF. Equations (28) and (29) express the generic non-linear model used for the state estimation process.

$$\frac{dx(t)}{dt} = f(x(t), u(t)) + w(t) \tag{28}$$

$$y = h(x(t)) + v(t) \tag{29}$$

where $w(t)$ and $v(t)$ denote noise and measurement noise, respectively.

*EKF Algorithm*

EKF algorithm is established to provide sensorless control that is required for state estimation. The implementation of the filter state-space model of the motor is required. After knowing state matrices, it is required to calculate the state transition matrix and prediction state. By minimizing the estimation error covariance, optimality of the estimated state is achieved. Initialization, prediction, and correction are involved in the EKF process to estimate torque, speed, and flux. The extended state variables vector of the induction motor can be defined as given in (30).

$$\begin{bmatrix} x_1(t) \\ x_2(t) \\ x_3(t) \\ x_4(t) \\ x_5(t) \\ x_6(t) \end{bmatrix} = \begin{bmatrix} i_{s\alpha} \\ i_{s\beta} \\ \psi_{s\alpha} \\ \psi_{s\beta} \\ \omega_r \\ T_L \end{bmatrix} \tag{30}$$

The filter uses the current estimation of inputs and states. f is the nonlinear function of the states and input. Input u is the alpha and beta components of stator voltage. Linearization is done by using (31). Function $F(t)$ and $H(t)$ are the Jacobians. $\hat{x}(t) = E(x(t))$ is the state space model whose states are estimated at t.

$$F(t) = \frac{\partial f}{\partial x}(\hat{x}(t), u(t)) \tag{31}$$

$$H(t) = \frac{\partial h}{\partial x}(\hat{x}(t)) = \begin{bmatrix} 1 & 0 & 0 & 0 & 0 & 0 \\ 0 & 1 & 0 & 0 & 0 & 0 \end{bmatrix} \tag{32}$$

Using $F$, the error covariance matrix is calculated as given in Equation (33). Initially, the value of the error covariance matrix P is set to zero. Matrices $Q$ and $R$ are defined in (34).

$$\dot{P}_c(t) = F(t)P_c(t) + P_c(t)F(t)^T - K(t)H(t)P_c(t) + Q(t) \tag{33}$$

where $K(t) = P_c(t)H(t)^T R(t)^{-1}$.

System parameter values and covariance matrix are very important and effective on the states estimation accuracy. Computational complexity avoided by covariance matrices of measurement and system noises is chosen in diagonal form. These matrices are obtained by considering the stochastic properties of noises [36,37]. The choice of $R$ and $Q$ matrix in EKF filter design is significant. For state estimation design of the $Q$ matrix is very crucial as it affects the estimation error, and it is a weighting matrix. The literature proves that the solution to the Riccati equation for error covariance is a first-order approximation. So, when the system is linearized, then it is noisier than the non-linear system. So, tuning the $Q$ matrix is very critical. From the stability property of EKF, if the value of the $Q$ matrix is

positive definite, then the Controllability Gramian of $(F, Q)$ is bounded and also positive definite. This property for a non-linear system like our system helps in selecting the $Q$ matrix. This results in less estimation error. From the literature on control, an increase in cost is inversely proportional to response speed. $Q$ is tuned by adding a manual weight of less than 50, which results in a significant estimation error. After that, it is increased, which results in a decrease in error. Thus, this trial-and-error method is used to achieve the desired state estimation with minimum error. Matrices $Q$ and $R$ are covariance matrices of $w(t)$ and $v(t)$ which are given in Equation (34). Figure 4 shows the structure of extended Kalman filter.

$$R = \begin{bmatrix} 1 & 0 \\ 0 & 1 \end{bmatrix}, Q = \begin{bmatrix} \alpha & 0 & 0 & 0 & 0 & 0 \\ 0 & \alpha & 0 & 0 & 0 & 0 \\ 0 & 0 & \alpha & 0 & 0 & 0 \\ 0 & 0 & 0 & \alpha & 0 & 0 \\ 0 & 0 & 0 & 0 & \alpha_1 & 0 \\ 0 & 0 & 0 & 0 & 0 & \alpha_1 \end{bmatrix} \tag{34}$$

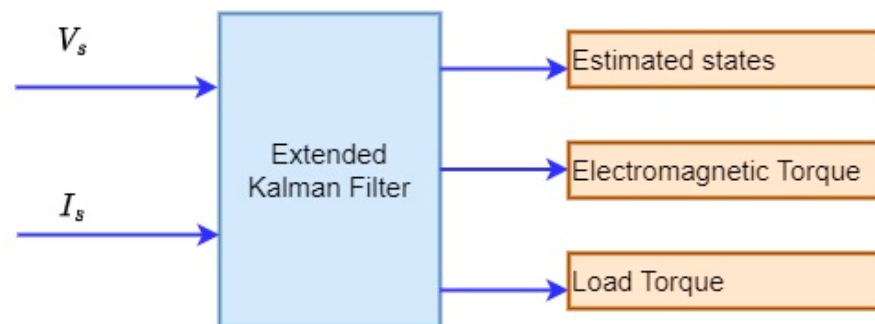where $\alpha = 104$ and $\alpha_1 = 105$.



**Figure 4.** Structure of EKF.

## 6. Space Vector Modulation

A three-phase bridge inverter is used after modulation with eight switching states, and for all states, a corresponding voltage vector is generated. Figure 5 shows all switching states. For the three-phase, we have a revolving reference voltage vector that rotates in each sector. If this vector is in sector 1, voltage vector 1 and 2 is applied according to their application time by resolving it into their components. The rest of the time, the null/zero vector is applied, so the concept of the average voltage vector is applied in SVM over a sub-cycle Ts. Application time T1, T2, and T0 of the reference vector is shown below.

$$T_1 = \frac{T_s}{2V_{dc}} \left( \sqrt{6} V_{s\beta ref} - \sqrt{2} V_{s\alpha ref} \right) \tag{35}$$

$$T_2 = \sqrt{2} \frac{T_s}{V_{dc}} \left( V_{s\alpha ref} \right) \tag{36}$$
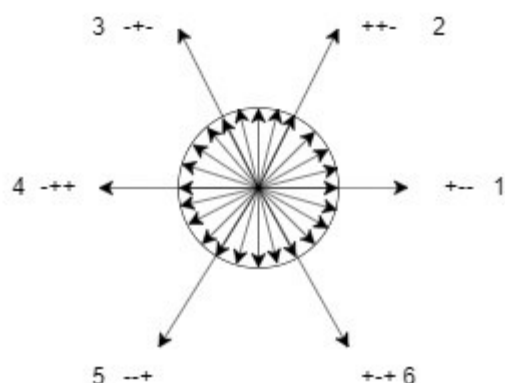
$$T_o = T_s - (T_1 + T_2) \tag{37}$$

**Figure 5.** Space vector modulation.

### 7. Results and Discussion

The proposed control scheme has been implemented in MATLAB/Simulink and results have been presented in this section. The speed control test for the proposed controller has been done for four different cases. The reference inputs for all the cases have been discussed as follows:

1. Motor speed has been changed from 0 Revolutions per Minute (RPM) to 1000 RPM using a step function,
2. Motor speed is changed from 0 to 1000 RPM using a step signal and then it is suddenly reversed to $-1000$ RPM, i.e., it operated to 1000 RPM in opposite direction,
3. Motor speed is kept constant for 0.5 s and is then increased linearly with time to 487 RPM,
4. Motor speed is kept constant at 0 RPM for 1 s and then is increased to 500 RPM. It is kept constant at that speed for 1.5 s and is then suddenly increased to 1400 RPM. After keeping constant at 1400 RPM, it has been decreased to 0 RMP and is then increased to 500 RPM after being kept constant for 1 s.

The controller parameters for FOPID controllers are given in Table 3. It should be mentioned here that the comparison of results for the FOPID controller has been done with the PI controller proposed in [25].

**Table 3.** Controller parameters.

| Controller Parameters for Speed | |
|---|---|
| $K_p$ | 2 |
| $K_i$ | 0.01 |
| $\lambda$ | 0.92 |
| $K_d$ | 0.01 |
| $\mu$ | 0.85 |
| Controller Parameters for Torque | |
| $K_p$ | 1000 |
| $K_i$ | 100 |
| $\lambda$ | 0.9 |
| $K_d$ | 0 |
| $\mu$ | 0 |
| Controller Parameters for Flux | |
| $K_p$ | 0.5 |
| $K_i$ | 1 |
| $\lambda$ | 0.9 |
| $K_d$ | 0.01 |
| $\mu$ | 0.2 |

The controllers along with the EKF have been applied in the closed loop system as shown in Figure 2 and the simulation results have been obtained. The motor was provided a reference speed of 1000 RPM to track. The electromagnetic torque of the motor generated subjected to 1000 RPM reference speed is shown in Figure 6.
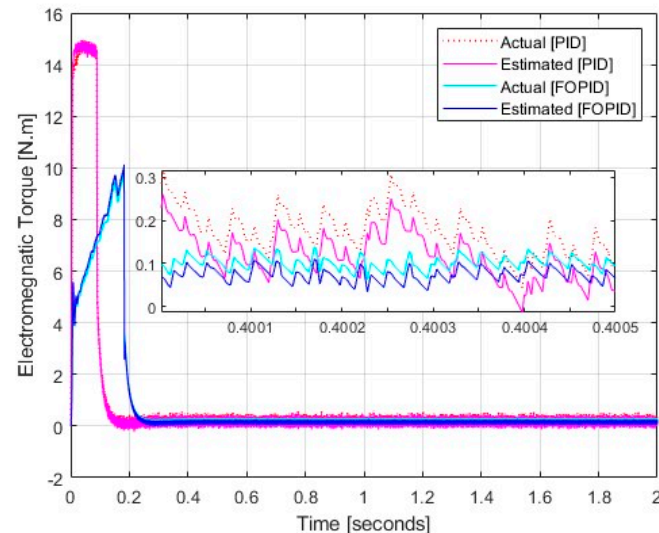


**Figure 6.** Electromagnetic torque.

It can be seen from Figure 6 that the torque generated by applying the PID controller has a peak of almost 15 Nm and then it decays down to almost 0. While the torque generated by the application of the FOPID controller has a peak of 10 Nm and then decays down to 0 Nm. It should be noted that the actual electromagnetic torque and the one estimated through EKF have the same profiles for both PID and FOPID controllers. It should also be noted that the ripple magnitude in electromagnetic torque produced with the FOPID controller has been reduced by almost one-third as compared to that with the PID controller. Figure 7 represents the stator flux magnitude, both actual and estimated through EKF, for the FOPID controller.
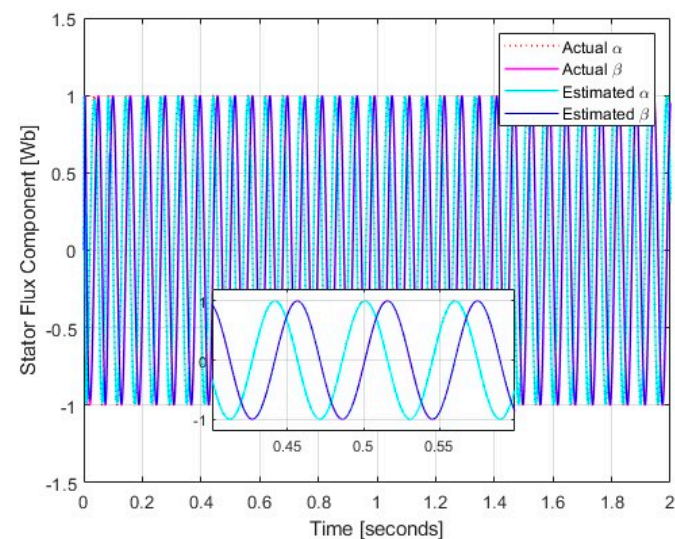


**Figure 7.** Stator flux components.

The stator flux magnitude for the induction motor in Figure 7 shows smooth sinusoidal variations for both flux components $\alpha$ and $\beta$. It should also be noted that the flux components for actual and estimated magnitudes are the same. The absence of ripples

is evident in the effectiveness FOPID controller. Figure 8 shows the flux profile for the 1000 RPM reference speed of the motor. Moreover, it can be seen from Figure 7 that the flux has a faster tracking response with no ripples.
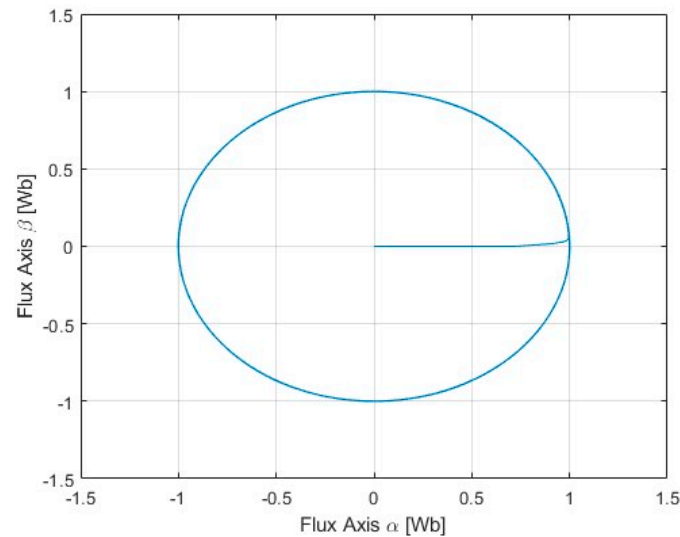


**Figure 8.** Stator flux circular trajectory.

The speed control for different reference trajectories with PID and FOPID controllers for speed variations discussed above is shown in Figure 9. At the outset, it can be stated that the proposed approach has been able to minimize high-frequency ripples from torque and stator flux of the IM as shown in Figures 6 and 7.
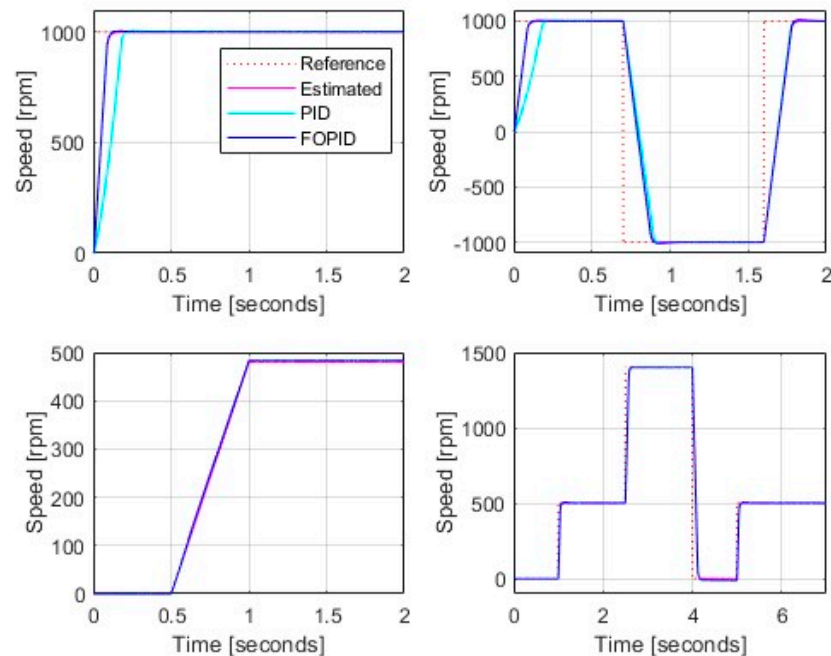


**Figure 9.** Rotor speed variations subjected to different reference trajectories.

It is evident from Figure 9 that the actual and estimated rotor speeds, using EKF with FOPID controller, of the induction motor are the same. However, the top two subplots of Figure 9 show that the FOPID controller ensures fast-tracking of the reference speed compared to the PID controller. It should also be noted that there is no overshoot in rotor speed for both PID and FOPID controllers. The increased time delay for the FOPID

controller in speed tracking for the top-right subplot is because the reference trajectory has been designed such that rotor speed suddenly changes from 1000 RPM to −1000 RMP, i.e., the direction of movement of the rotor has been reversed while keeping the speed constant which is physically impossible. So, what the proposed control strategy does is that it reduces speed from 1000 RPM to 0 and then changes its direction and thereby reaching a speed of −1000 RPM. The speed tracking with PID and FOPID controllers for reference trajectories in the lower two cases of Figure 9 is the same.

The final comparison between the proposed control scheme and the sliding mode is presented in Table 4. The error between real and estimated states of torque, flux, and speed is presented. The error in flux and torque estimation is negligible, which shows that states are estimated with accuracy. Speed error is steadily decreasing with time and approaches zero. From Table 4, it can be seen that both techniques have 0% overshoot. However, when discussing the time delay parameter, it is clear from Table 4 that the presented technique shows its superiority.

**Table 4.** Comparative analysis of speed and Tracking error.

| Speed Range | Time (s) | Time Delay (s) | | Percent Overshoot | | Comments |
|---|---|---|---|---|---|---|
| | | FOPID | PID | FOPID | PID | |
| 0–1000 | 0 to 0.7 | 0.1 | 0.1 | 0% | 0% | Time delay same |
| 1000 to 1000 | 0.7 to 1.6 | 0.2 | 0.27 | 0% | 0% | Time delay of EKF is less (0.07 s) |
| −1000 to 1000 | 1.6 to 2 | 0.2 | 0.27 | 0% | 0% | Time delay of EKF is less (0.07 s) |
| 0 to 1000 | 0 to 0.7 | 0.07 | 0.1 | 0% | 0% | Time delay of EKF is less (0.03 s) |
| 100 to 600 | 0.7 to 1.4 | 0.02 | 0.45 | 0% | 0% | Time delay of EKF is less (0.43 s) |
| 600 to 1000 | 1.4 to 2 | 0.02 | 0.4 | 0% | 0% | Time delay of EKF is less (0.38 s) |
| 0 to 480 | 0 to 1 | | | 0% | | |
| 480 to 1430 | 1 to 2.5 | | | 0% | | This analysis is for a wide speed range. Less |
| 1430 to 0 | 2.5 to 4 | 0 | 0 | 0% | 0 | time delay for speed tracking highlights the |
| 0–1430 | 4 to 5 | | | 0% | | fast performance of the proposed scheme. |
| 1430 to 480 | 5 to 7 | | | 0% | | |

Although a FOPID controller, due to two additional tunable parameters, provided more degree of freedom in control design, an integer order approximation of the fractional transfer function is required for hardware implementation. Higher integer order approximation results in higher accuracy and thus the computation complexity is increased. In the future, the supercapacitors may be designed to approximate the fractional derivatives to improve the hardware implementation complexity of the fractional order PID controllers.

A comparison of the proposed approach with others presented in the literature with respect to the time delay and percent overshoot has been given in Table 5. It is clear from Table 5 that the proposed approach not only supersedes the others in terms of a fast response, but it also has no overshoot in reference tracking of rotor speed.

**Table 5.** Comparison with existing techniques with no load.

| Approach | Time Delay (s) | % Overshoot |
|---|---|---|
| Proportional integral (PI) + Slide Mode Observer (SMO) [25] | 0.1 | 0% |
| Direct Torque Control (DTC) + Slide Mode Control (SMC) [38] | 0.17 | 6.385% |
| PI + Space Vector Modulation (SVM)-DTC [39,40] | 0.095 | 0% |
| Proposed technique (FOPID + extended Kalman filter (EKF)) | 0.07 | 0% |

## 8. Conclusions

A non-integer differential-integral equations-based control strategy has been proposed for sensorless speed control of an induction motor. The idea is to control the rotor speed without its direct measurements at the output. So, an EKF has been designed to estimate the motor speed using torque and flux magnitudes. EKF successfully estimates the rotor speed

and its comparison with the actual value shows negligible error. Since the torque magnitude when controlled through a PI controller has ripple magnitudes and derivative action can be a source of uncertainty due to high-frequency noise, fractional order derivatives, and integrals are used to design the controller. This non-integral order PID controller used along with SVM not only ensures speed tracking with negligible time delay, but it also minimizes the ripples to almost one-fourth magnitude as compared to that with PI controller. This work uses three different fractional order controllers for flux, torque, and speed control which requires their separate implementation when connected to hardware in a real-time system. This limitation may be eliminated in the future by designing a centralized controller to ensure torque, flux, and speed control and minimize the ripples magnitude at the same time.

**Author Contributions:** Conceptualization, T.N. and A.A.; methodology, A.A., M.U.C. and I.u.H.S.; software, T.N., D.N. and M.M.I.; validation, A.A., D.N., M.M.I. and V.B.; formal analysis, M.U.C., D.N., V.B. and V.P.; investigation, T.N., A.A., D.N. and S.K.; resources, A.A., M.U.C., I.u.H.S. and V.B.; data curation, T.N., A.A., D.N., I.u.H.S. and V.B.; writing—original draft preparation, T.N., A.A., I.u.H.S. and S.K.; writing—review and editing, D.N., V.B., M.M.I. and V.P.; visualization, T.N., M.M.I. and S.K.; supervision, A.A. and I.u.H.S.; project administration, M.U.C.; funding acquisition, M.U.C., V.B. and V.P. All authors have read and agreed to the published version of the manuscript.

**Data Availability Statement:** No new data were created or analyzed in this study. Data sharing is not applicable to this article.

**Conflicts of Interest:** The authors declare no conflict of interest.

## References

1. Kolhe, M.S.; Tapre, M.P.C. Condition Monitoring & Control of Induction Motors by using IoT Platform for Agriculture System. *Int. J. Eng. Res. Technol.* **2019**, *8*, 1043–1045.
2. Ramesh, A.; Kumar, M.S.; Sekhar, O.C. Interleaved boost converter fed with PV for induction motor/agricultural applications. *Int. J. Power Electron. Drive Syst.* **2016**, *7*, 835. [CrossRef]
3. Martins, C.A.; Carvalho, A.S. Technological trends in induction motor electrical drives. *IEEE Porto Power Tech Proc.* **2001**, *2*, 7.
4. Behrooz, F.; Mariun, N.; Marhaban, M.H.; Radzi, M.A.M.; Ramli, A.R. Review of control techniques for HVAC systems—Nonlinearity approaches based on Fuzzy cognitive maps. *Energies* **2018**, *11*, 495. [CrossRef]
5. El Ouanjli, N.; Derouich, A.; El Ghzizal, A. Modern improvement techniques of direct torque control for induction motor drives-a review. *Prot. Control Mod. Power Syst.* **2019**, *4*, 1–12. [CrossRef]
6. Vas, P.; Alakula, M. Field-oriented control of saturated induction machines. *IEEE Trans. Energy Convers.* **1990**, *5*, 218–224. [CrossRef]
7. Depenbrock, M. Direct self-control (DSC) of inverter fed induktion machine. *IEEE Power Electron. Spec. Conf.* **1987**, *3*, 632–641.
8. Takahashi, I.; Noguchi, T. A new quick-response and high-efficiency control strategy of an induction motor. *IEEE Trans. Ind. Appl.* **1986**, *5*, 820–827. [CrossRef]
9. Casadei, D.; Profumo, F.; Serra, G.; Tani, A. FOC and DTC: Two viable schemes for induction motors torque control. *IEEE Trans. Power Electron.* **2002**, *17*, 779–787. [CrossRef]
10. Lai, Y.-S.; Chen, J.-H. A new approach to direct torque control of induction motor drives for constant inverter switching frequency and torque ripple reduction. *IEEE Trans. Energy Convers.* **2001**, *16*, 220–227.
11. Lin, F.-J.; Wai, R.-J. Hybrid control using recurrent fuzzy neural network for linear induction motor servo drive. *IEEE Trans. Fuzzy Syst.* **2001**, *9*, 102–115.
12. Ahn, T.-C.; Kwon, Y.-W.; Hwang, H.-S.; Pedrycz, W. Design of neuro-fuzzy controller on DSP for real-time control of induction motors. In Proceedings of the 9th IFSA World Congress and 20th NAFIPS International Conference, Vancouver, BC, Canada, 25–28 July 2002; pp. 3038–3043.
13. Moallem, M.; Mirzaeian, B.; Mohammed, O.A.; Lucas, C. Multi-objective genetic-fuzzy optimal design of PI controller in the indirect field oriented control of an induction motor. *IEEE Trans. Magn.* **2001**, *37*, 3608–3612. [CrossRef]
14. Habibullah, M.; Lu, D.D.-C.; Xiao, D.; Rahman, M.F. A simplified finite-state predictive direct torque control for induction motor drive. *IEEE Trans. Ind. Electron.* **2016**, *63*, 3964–3975. [CrossRef]
15. Wróbel, K.; Serkies, P.; Szabat, K. Model predictive base direct speed control of induction motor drive—Continuous and finite set approaches. *Energies* **2020**, *13*, 1193. [CrossRef]

16. Ammar, A.; Bourek, A.; Benakcha, A. Modified load angle Direct Torque Control for sensorless induction motor using sliding mode flux observer. In Proceedings of the 4th International Conference on Electrical Engineering (ICEE), Boumerdes, Algeria, 13–15 December 2015; pp. 1–6.
17. Azcue-Puma, J.L.; Filho, A.J.S.; Ruppert, E. The fuzzy logic-based stator-flux-oriented direct torque control for three-phase asynchronous motor. *J. Control Autom. Electr. Syst.* **2014**, *25*, 46–54. [CrossRef]
18. Barambones, O.; Alkorta, P. Position control of the induction motor using an adaptive sliding-mode controller and observers. *IEEE Trans. Ind. Electron.* **2014**, *61*, 6556–6565. [CrossRef]
19. Zelechowski, M.; Kazmierkowski, M.P.; Blaabjerg, F. Controller design for direct torque controlled space vector modulated (DTC-SVM) induction motor drives. In Proceedings of the IEEE International Symposium on Industrial Electronics, Dubrovnik, Croatia, 20–23 June 2005; Volume 3, pp. 951–956.
20. Ferdiansyah, I.; Rusli, M.R.; Praharsena, B.; Toar, H.; Purwanto, E. Speed control of three phase induction motor using indirect field oriented control based on real-time control system. In Proceedings of the 10th International Conference on Information Technology and Electrical Engineering (ICITEE), Bali, Indonesia, 24–26 July 2018; pp. 438–442.
21. Manes, C.; Parasiliti, F.; Tursini, M. A comparative study of rotor flux estimation in induction motors with a nonlinear observer and the extended Kalman filter. In Proceedings of the IECON'94–20th Annual Conference of IEEE Industrial Electronics, Bologna, Italy, 5–9 September 1994; Volume 3, pp. 2149–2154.
22. Lascu, C.; Boldea, I.; Blaabjerg, F. Direct torque control of sensorless induction motor drives: A sliding-mode approach. *IEEE Trans. Ind. Appl.* **2004**, *40*, 582–590. [CrossRef]
23. Talla, J.; Leu, V.Q.; Šmídl, V.; Peroutka, Z. Adaptive speed control of induction motor drive with inaccurate model. *IEEE Trans. Ind. Electron.* **2018**, *65*, 8532–8542. [CrossRef]
24. Traoré, D.; Plestan, F.; Glumineau, A.; De Leon, J. Sensorless induction motor: High-order sliding-mode controller and adaptive interconnected observer. *IEEE Trans. Ind. Electron.* **2008**, *55*, 3818–3827. [CrossRef]
25. Ammar, A.; Bourek, A.; Benakcha, A. Sensorless SVM-direct torque control for induction motor drive using sliding mode observers. *J. Control Autom. Electr. Syst.* **2017**, *28*, 189–202. [CrossRef]
26. Zhou, M.; Cheng, S.; Feng, Y.; Xu, W.; Wang, L.; Cai, W. Full-Order Terminal Sliding-Mode-Based Sensorless Control of Induction Motor with Gain Adaptation. *IEEE J. Emerg. Sel. Top. Power Electron.* **2021**, *10*, 1978–1991. [CrossRef]
27. Liu, P.; Hung, C.-Y.; Chiu, C.-S.; Lian, K.-Y. Sensorless linear induction motor speed tracking using fuzzy observers. *IET Electr. Power Appl.* **2011**, *5*, 325–334. [CrossRef]
28. Cai, X.; Wang, Q.; Wang, Y.; Zhang, L. Research on a Variable-Leakage-Flux Permanent Magnet Motor Control System Based on an Adaptive Tracking Estimator. *Energies* **2023**, *16*, 587. [CrossRef]
29. Alsofyani, I.M.; Idris, N.R.N. Simple flux regulation for improving state estimation at very low and zero speed of a speed sensorless direct torque control of an induction motor. *IEEE Trans. Power Electron.* **2015**, *31*, 3027–3035. [CrossRef]
30. Chapman, S.J. *Electric Machinery Fundamentals*; McGraw-Hill: New York, NY, USA, 2004.
31. Zamani, M.; Karimi-Ghartemani, M.; Sadati, N.; Parniani, M. Design of a fractional order PID controller for an AVR using particle swarm optimization. *Control Eng. Pract.* **2009**, *17*, 1380–1387. [CrossRef]
32. Bingül, Z.; Karahan, O. Fractional PID controllers tuned by evolutionary algorithms for robot trajectory control. *Turk. J. Electr. Eng. Comput. Sci.* **2012**, *20*, 1123–1136. [CrossRef]
33. Rajasekhar, A.; Jatoth, R.K.; Abraham, A. Design of intelligent PID/PIλDμ speed controller for chopper fed DC motor drive using opposition based artificial bee colony algorithm. *Eng. Appl. Artif. Intell.* **2014**, *29*, 13–32. [CrossRef]
34. Podlubny, I. Fractional-order systems and PI/sup/spl lambda//D/sup/spl mu//-controllers. *IEEE Trans. Automat. Contr.* **1999**, *44*, 208–214. [CrossRef]
35. Bingul, Z.; Karahan, O. Comparison of PID and FOPID controllers tuned by PSO and ABC algorithms for unstable and integrating systems with time delay. *Optim. Control Appl. Methods* **2018**, *39*, 1431–1450. [CrossRef]
36. Vas, P. *Sensorless Vector and Direct Torque Control*; Oxford University Press: New York, NY, USA, 1998.
37. Ge, Q.; Feng, Z. Speed estimated for vector control of induction motor using reduced-order extended Kalman filter. In Proceedings of the Third International Power Electronics and Motion Control Conference, Beijing, China, 15–18 January 2000; pp. 138–142.
38. El Daoudi, S.; Lazrak, L.; Lafkih, M.A. Sliding mode approach applied to sensorless direct torque control of cage asynchronous motor via multi-level inverter. *Prot. Control Mod. Power Syst.* **2020**, *5*, 1–10. [CrossRef]
39. Ammar, A.; Benakcha, A.; Bourek, A. Closed loop torque SVM-DTC based on robust super twisting speed controller for induction motor drive with efficiency optimization. *Int. J. Hydrogen Energy* **2017**, *42*, 17940–17952. [CrossRef]
40. Premkumar, K.; Thamizhselvan, T.; Priya, M.V.; Carter, S.B.R.; Sivakumar, L.P. Fuzzy anti-windup pid controlled induction motor. *Int. J. Eng. Adv. Technol.* **2019**, *9*, 184–189. [CrossRef]